STATUS OF UA9, THE CRYSTAL COLLIMATION EXPERIMENT IN THE SPS*

W. Scandale[#], CERN, Geneva, CH, LAL, Orsay, Fr, INFN, Roma1,It for the UA9 Collaboration.

Abstract

UA9 was operated at the CERN-SPS for more than two years to investigate the feasibility of halo collimation with bent crystals. Silicon crystals 2 mm long with bending angles of about 170 µrad were used as primary collimators. The crystal collimation process was steadily achieved through channeling, with high efficiency. The crystal orientation was easily set and optimized with an installed goniometer that has an angular accuracy of about ± 10 µrad. In channeling orientation, the loss rate of the halo particles interacting with the crystal is reduced by half an order of magnitude, whilst the residual off-momentum halo escaping from the crystal-collimator area is reduced by a factor two to five. The crystal channeling efficiency of about 75% is reasonably consistent with simulations and with single pass data collected in the extracted proton beam of the SPS North Experimental Area. The accumulated observations, shown in this paper, support our expectation that the coherent deflection of the beam halo by a bent crystal should help considerably in enhancing the collimation efficiency in LHC.

INTRODUCTION

Halo particles surrounding the beam core in a circular accelerator are a threat for performance and machine protection. To collimate them a cascade of movable passive targets is used. The collimation system built for LHC that has recently reached unprecedented performance is a sophisticated setup made of four primary scattering targets and several secondary absorbers [1]. Bent crystals installed upstream of the collimation system should reduce its inefficiency by another order of magnitude [2]. Amorphous primary targets scatter particles in no preferred direction while bent crystals trap particles on aligned atomic planes and kick them in only one direction. The halo can thus be redirected onto the secondary absorber with a larger impact parameter and removed more efficiently. Particles in channeling states travel far from the lattice nuclei, which results in reduced nuclear interaction rate and smaller energy loss. The halo population escaping collimation and, in particular, the off-momentum part of it decreases with reduced risk of irradiating sensitive devices especially in dispersive areas.

Successful attempts to extract halo particles with bent crystals were made at CERN in the 1990s, IHEP-Protvino, RHIC and FNAL. However, none of them could provide compelling evidence that crystal-assisted collimation is feasible in modern hadron colliders [3].

The UA9 experiment started in 2008 at the SPS to investigate if crystal-assisted collimation can be an alternative for protons and lead ion collimation in LHC. The aim is to demonstrate that crystal-based collimation

has higher efficiency than traditional scheme. This paper reports the experimental evidence collected in 2010.

EXPERIMENTAL APPARATUS

Fig. 1 shows the schematic layout of UA9 installed in the straight section 5 of the SPS [4]. Two stations at 90° phase advance and at large values of the horizontal beta function reproduce a two-stage horizontal collimation setup that sits close to the quadrupoles QF1 and QF2, respectively. The first station contains four crystals C1 to C4. Each of them, mounted on a mechanical goniometer, can be moved close to the beam core and oriented parallel to the halo particle trajectory thus acting as primary collimator. The second station located 60 m downstream contains a 60 cm long tungsten absorber (TAL) that can be moved towards the beam core to collect the deflected halo particles thus acting as secondary collimator.

Figure 1: Schematic layout UA9.

About 40 m downstream of the crystals there is an LHC-type collimator (COL) made of two-sided copper jaws 1 m long that can be moved horizontally to precisely define the beam envelope and identify the beam orbit center. The collimator is also used to scan the deflected beam. The showers induced by the intercepted flux are seen by a beam loss monitor (BLM) downstream and give information about the deflecting angle and the channeling efficiency of the crystal. A Roman Pot is installed after the collimator: it comprises two horizontal axes with linear motors, each supporting a secondary vacuum vessel with a Medipix detector MED made of square 55 µm pixels. The detector can be moved towards the pipe axis to intercept the deflected beam, thus providing an online image of the beam.

About 120 m downstream of the crystals the dispersion function increases to its maximal value. Limiting aperture devices (TAL2) are located there for optimal detection of the off-momentum halo escaping from the collimation stations. The escape mechanism is inherent to the collimation process. Single diffractive events in the primary collimator may leave the trajectory unchanged and substantially reduce the energy of the incident particles, thereby preventing the secondary absorber from collecting them. Those particles have larger orbit deviations as the dispersion function increases. The deviation is maximal at the TAL2 position. In bent crystals, ionization energy loss and nuclear interactions are substantially reduced [5]. So should be the diffractive

04 Hadron Accelerators

interactions and the population of self-generated off-momentum halo. One of the main goals of UA9 is to measure such a reduction in the TAL2 area. Two horizontally movable devices in the inner side of the SPS ring can intercept and evaluate the secondary halo population escaping collimation. A 10 cm long duralumin bar (SC) is used as a scraper and a BLM downstream is used to evaluate the incoming flux. A Cherenkov detector (CH) nearby can scan and count the intercepted flux.

Scintillation counters such as SB and SL close to the crystals and SJ and SK close to TAL2 are used to detect local losses generated in strategic areas of the beam line.

UA9 crystals are optimized for collimation [3]. They are made of dislocation-free silicon crystal plates etched and optically polished. The face intercepting the beam at small grazing angles has a few mm length and constant curvature whilst amorphous layer, miscut angle with the crystal planes and residual torsion are minimal to favor channeling efficiency. C1 and C4 are strip crystals cut along the (110) planes, mounted on a mechanical holder that imparts a flexural stress to the strip axis inducing an orthogonal anticlastic curvature. C2 and C3 are thin plates cut along the (111) planes, in which the 3D elastic reaction to the flexural stress of the largest face induces an orthogonal anticlastic reaction and a quasi-mosaic bend of the thin face exposed to beam halo. Performance of C1 and C2 is reported in [6] and no longer discussed here. Table 1 shows parameters of C3 and C4 that are mounted on a two-arm goniometer, built at IHEP with ±10 μrad angular accuracy.

Table 1: Crystal parameters

Crystal	Length (mm)	Angle (μrad)		Torsion (μrad/mm)
		Bend	Miscut	
C3	2.1	165	90	1
C4	2.0	176	200	0.6 – 1.0

EXPERIMENTAL RESULTS

During the UA9 runs the SPS beam energy was 120 GeV and occasionally 270 GeV. The beam was typically made of a single bunch with a few 10^9 - 10^{11} protons or Pb ions with a lifetime of a few minutes to 10 hours, depending on the selected distance of the primary crystal from the beam closed orbit. The number of particles hitting the crystal was in the range 10 - 10^3 protons per turn, all within a bunch length of a few ns. The average amplitude growth of particle oscillations was smaller than 0.1 nm per turn. The massive COL jaws were used to align the relative positions of all UA9 movable elements to the specific closed orbit of each run. In collimation operation, one of the crystals was the primary obstacle for the beam halo at about 3-6 σ_x from the beam closed orbit, while the TAL was located a couple of σ_x further away, with σ_x being the RMS horizontal beam size.

Figure 2 shows the response of the beam loss monitor to an angular scan of C3 in a crystal collimation run.

Curve 1 shows the dependence of the loss count on the orientation of C3 and is in good agreement with curve 2 resulting from a simulation [7]. The dot-dashed line corresponds to the relative loss rate for amorphous orientations of the crystal to which curves 1 are 2 are normalized. The angle origin is chosen at the minimum of curve 1. For this orientation the fraction of beam halo deflected by the crystal in channeling states is maximal, the inelastic interactions in the crystal are minimal and the beam loss rate decreases by a factor 5 with respect to the amorphous orientations. An angular scan of Fig.2 is the optimal way to find the best orientation for channeling. Indeed, simulations show that around the loss minimum the channeling efficiency varies slowly whilst the inelastic interaction probability varies very strongly. On the right of the loss minimum, there is a wide angular range of significant beam loss reduction due to volume reflection (VR) of halo particles in the crystal. Its width equals the crystal bend angle. The kick due to VR is θ_{vr}=22 μrad whilst the multiple scattering RMS angle is θ_{ms}=14 μrad. In VR the particles thus perform a smaller number of passages through the crystal to reach the TAL aperture than for amorphous orientations. This reduces the total number of inelastic interaction losses in the crystal. The channeling minimum in curve 1 is not as deep as in curve 2 whilst curve 2 exceeds curve 1 in most of the VR range. The origin of the discrepancy is not yet explained. Threefold effects are yet unaccounted in simulations. The miscut angle can modify particle trajectories with a very small impact parameter during multi-turn crystal hits [8]. Larger channeling inefficiency may appear at the crystal edges due to the fabrication process. Multi-turn halo population increases when rotating the crystal from amorphous to channeling orientation.
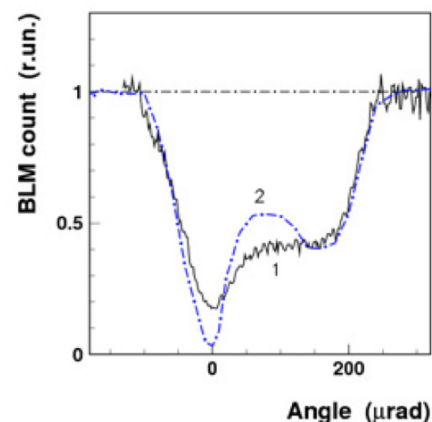

Figure 2: Angular scan of the crystal C3. (1) Observed and (2) simulated loss rate dependence on the crystal orientation. The dot-dashed line refers to amorphous orientation of the crystal.

The beam halo fraction escaping from the collimation area was estimated with the TAL2 devices. Scans were made from the garage position to the beam edge. Fig. 3 shows the dependence of the BLM count on the

04 Hadron Accelerators

T19 Collimation

horizontal position of the SC jaw during two such scans made with C3 in amorphous (AM) and channeling (CH) orientations. Two arrows indicate the projection of the TAL and C3 innermost edge at the TAL2 azimuth. Particles intercepted behind the TAL shadow should have escaped from collimation with negative off-momentum values. Their population was reduced by a factor of 2 (Fig. 3) to 5 (data not reported here) when rotating C3 from amorphous to channeling orientation.
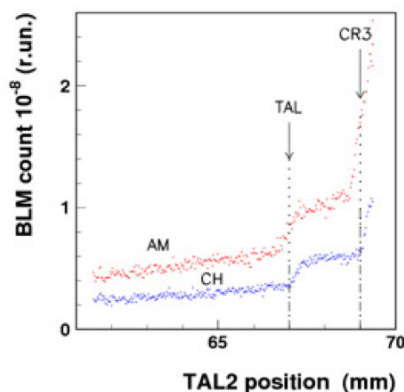

Figure 3: Dependence of beam loss monitor signal normalized to beam intensity on the horizontal position of the scraper (SC) in the high dispersion area behind the collimator-absorber. SC moves towards the beam periphery. CR3 is in amorphous (AM) or in channeling (CH) orientation. The arrows are the projections of the TAL and C3 inner edge at the SC position.

The beam halo fraction deflected by C3 in channeling mode was measured by intersecting the deflected beam either with the COL or with the MED in the Roman pot. Its value was found to be 80% [6].

Similar experiments were performed using Pb ion beams at 120 GeV per charge [8]. Channeling performance is the same as for protons, except that ionization losses and nuclear interaction rates are larger. In a 2 mm long silicon crystal in amorphous orientation the mean energy loss is 1.05 MeV for protons and 6.59 GeV for Pb ions, corresponding to relative off-momentum δ_p=-8.7×10^{-6} and δ_{Pb}=-0.66×10^{-3}. For a bucket half-height δ_h=1.54×10^{-3}, three passages through the nonaligned crystal were on average sufficient to debunch the Pb ion beam. The total cross-section for inelastic nuclear interactions and electromagnetic dissociation of Pb ion in silicon, $\sigma_{tot}=\sigma_h+\sigma_{ed}$=4.323+1.091=5.414 b, is 10 times larger than for protons. The attenuation length is 3.76 cm, thus about 5% of the Pb ions is lost per crystal traversal. Angular scans with Pb ions were thus expected to give a flatter response than with protons. In crystal C3, the loss rate reduction factor for Pb ions was 1.2 in the VR plateau and 2.5 in the channeling peak. In C4 the loss reduction factor was 1.4 in VR and 3.5 in channeling. Performance of C3 is worse than that of C4, because the deflecting planes (111) are non-equidistant. The width ratio of (111) channels is 3 and the most narrow of them are about 2.5 times smaller than (110) channels. Particles have a larger probability of inelastic interaction when travelling in the narrower channels. Simulations show that such a probability is 20% larger for C3 than in C4. They also show that the loss reduction factor in perfect channeling orientation is 8.3 and 14.2 for C3 and C4, respectively. For Pb ions, as for protons, there is a discrepancy between the experimental and simulation values of beam losses in channeling and VR orientations that may be due to surface imperfections and bad accounting of multi-turn halo population and of crystal miscut effects. The Pb ion beam halo fraction deflected by C3 in channeling states was measured by using a scan of the COL jaws [6]. Its value was found to be 74%. The off-momentum Pb ion fraction generated in the collimation process was also measured by scanning the beam periphery in the TAL2 station with the SC jaw and the Cherenkov detector. A factor 2 reduction of the halo population was observed in the absorber shadow when rotating the crystal from amorphous to channeling orientation.

CONCLUSIONS

UA9 results demonstrate that crystal collimation can be routinely achieved for proton and Pb ion beams with a robust and well-reproducible procedure. Its performance is superior to that of a standard collimation setup with amorphous primary target. The improvement is threefold. In channeling orientation, the channeling efficiency exceeds 75%, whilst the loss rate near the crystal and the off-momentum halo escaping from collimation devices are strongly reduced. The performance is inferior to that predicted by simulations for reasons not yet clarified. However the experimental evidence strongly supports an extended test of crystal collimation in LHC. Strip or quasi-mosaic crystals have equivalent performance, although strips are slightly better for Pb ions. The goniometer should be three times more accurate than in UA9, for faster and more reproducible orientation of the crystal at the higher energy in LHC. Other open issues are the crystal collimation performance at high intensity and halo flux rate, the robustness of the crystal and the absorber to high halo flux and the proper integration of the crystals in the existing LHC collimation system.

REFERENCES

[1] R.W. Assmann et al., "Designing and Building a Collimation System for the High-Intensity LHC Beam", PAC 03 Portland, Or, USA (2003).

[2] R. W. Assmann, S. Redaelli, W. Scandale, "Optics study for a possible crystal-based collimation system for the LHC", EPAC 06, Edinburgh (2006).

[3] W. Scandale, "Crystal-based collimation in modern hadron colliders", CERN-2009-04, p. 154 (2008).

[4] W. Scandale et al, "The UA9 experimental layout", submitted to JINST, Geneva (2011).

[5] W. Scandale et al., Nucl. Inst. and Methods B 268 (2010) 2655-2659.

[6] W.Scandale et al., Phys. Letters B 692 (2010) 78.

[7] W. Scandale and A. Taratin, CERN/AT 2008-21 (2008).

[8] W. Scandale et al., "Comparative Results on Collimation of the SPS Beam of Protons and Pb Ions with Bent Crystals", accepted for publication in PLB, Geneva (2011).